Program Digest, 2019 IEEE International Ultrasonics Symposium (IUS)
Glasgow, Scotland, October 6-9, 2019

Contrast-enhanced ultrasound imaging of acute changes in pancreatic cancer following targeted hyaluronan treatment

Ipek Oezdemir, Kulsoom Javed, Girdhari Rijal, Kenneth Hoyt*

Department of Bioengineering, University of Texas at Dallas, Richardson, TX, USA

* kenneth.hoyt@utdallas.edu

Abstract — **The purpose of this study was to monitor acute changes in pancreatic tumor perfusion with contrast-enhanced ultrasound (CEUS) imaging following targeted hyaluronan (HA) treatment. Intratumoral accumulation of HA is one of contributing factors that can lead to an increased tumor interstitial pressure (TIP). These elevated TIP levels can hinder delivery of chemotherapeutic drugs and cause treatment failure. For this study, pancreatic cancer-bearing mice were imaged at baseline and again at 2 h after intravenous administration of physiological saline (control group) or PEGPH20, which targets HA (therapy group). CEUS data were collected for 5 min and the temporal sequence was first analyzed using a singular value filter (SVF) to remove any background clutter signal. Given the time history of contrast agent flow, a tumor perfusion parametric analysis was performed. A series of morphological image operations was applied to quantify structural features of the tumor angiogenic network including vessel count, density, length, diameter, tortuosity, and branching points. After imaging, animals were euthanized, and tumors excised for histological processing. Acute microvascular changes were found at 2 h after drug administration as confirmed by CEUS imaging. Further, histologic analysis of tumor sections revealed lower HA accumulation in the therapy group animals. Overall, these findings suggest that CEUS imaging of acute changes in tumor perfusion may help identify an optimal window whereby follow-up chemotherapeutic drug dosing would be more effective.**

Keywords—cancer; hyaluronan; microbubble contrast agent; microvascular networks; ultrasound.

I. Introduction

Pancreatic cancer accounts for about 3% of all cancers in the US and about 7% of all cancer deaths [1]. Effective drug delivery to the bulk tumor can be profoundly impacted by excessive accumulation of hyaluronan (HA), which is a component of the extracellular matrix [2]. Increased HA is associated with high tumor interstitial pressure (TIP), and vascular collapse [3]–[6]. These physical conditions can compromise microvascular function and impede chemotherapeutic drug delivery. Recently, a PEGylated version of recombinant human hyaluronidase (PEGPH20) has been described. When administered systemically, PEGPH20 was shown to degrade HA levels in pancreatic cancer and improve drug delivery [4]–[8].

Real-time contrast-enhanced ultrasound (CEUS) is a noninvasive imaging technique that uses an intravascular tracer (microbubble, MB) to help visualize tumor microvascular networks [9]. These CEUS images can then be analyzed to extract both tumor perfusion and microvascular morphology features [10]–[14]. To that end, CEUS imaging has been used to assess the tumor response (or lack thereof) to gemcitabine plus PEGPH20 therapy [5]. This study revealed that this treatment protocol produced a positive response in pancreatic cancer-bearing mice after only one cycle of combination therapy. Consistent with known mechanisms, treated tumors exhibited decreased proliferation and increased apoptosis of primary cancer cells compared to placebo control. Using a novel image processing strategy applied to CEUS data, this paper aims to expand on earlier findings by evaluating the acute functional and structural changes of tumor microvasculature after administration of PEGPH20.

II. Methods

A. Animal Preparation and Imaging Protocol

All studies were approved by the Institutional Animal Care and Use Committee (IACUC) at the University of Texas at Dallas. Human BxPC3/HAS3 pancreatic cancer cells were implanted in the hindlimb (2 million per site near the tibia) of six-week-old male athymic nude mice (Charles River Laboratories, Wilmington, ME). Once tumors reached a size of 10 to 12 mm, animals were assigned to one of two groups, namely, control or therapy (N = 2 per). CEUS imaging of each tumor was performed using a clinical system (Acuson Sequoia 512, Siemens Healthcare, Mountain View, CA) equipped with a 15L8 linear transducer array. The transducer was fixed using a ring stand to maintain the same imaging plane during repeat measurements. Each animal received a 50 µL bolus injection of MBs (Definity, Lantheus Medical Imaging, N Billerica, MA) via a tail vein catheter. Using a MB sensitive imaging mode, a low transmit power (mechanical index, MI, less than 0.2) helped minimize contrast agent destruction.

This study was supported by National Institutes of Health (NIH) grants K25EB017222, R01EB025841, and Cancer Prevention Research Institute of Texas (CPRIT) grant RP180670.

TABLE I. FUNCTIONAL AND STRUCTURAL PARAMETER VALUES FOR EACH SUBJECT AND TIMEPOINT

Parameter	Control 1		Control 2		Therapy 1		Therapy 2	
	Baseline	2 h	Baseline	2 h	Baseline	2 h	Baseline	2 h
IPK	17.04	15.17	11.96	14.22	10.04	32.82	27.47	34.54
AUC	169.10	182.97	179.41	211.08	137.41	388.33	258.56	322.17
NB	0.00	0.00	5.00	6.00	0.00	8.00	0.00	4.00
NV	2.00	1.00	14.00	13.00	0.00	22.00	6.00	16.00
VD	0.00	0.00	0.07	0.03	0.00	0.10	0.01	0.05
VT	0.10	0.00	0.92	0.26	0.00	0.31	0.05	0.13
VL	22.07	1.00	38.59	17.19	0.00	19.55	11.87	14.20
MVD	0.01	0.01	0.08	0.03	0.00	0.13	0.02	0.06

[a] IPK = Peak intensity, AUC =Area under curve, NB = Number of vessels, NV = Number of vessels, VD = Vessel diameter, VT = Vessel tortuosity, VL = Vessel length, MVD = Microvessel density.

Each tumor was imaged by CEUS for 5 min at baseline and again at 2 h after systemic administration of a matched dose of saline (control) or PEGPH20 (therapy) (1.0 mg/kg, Halozyme Therapeutics, San Diego, CA). The body temperature of each animals was monitored during the entire study using a rectal probe regulated by a homeothermic controller (Kent Scientific Corp, Torrington, CT).

B. Image Processing

Sequences of CEUS images were first processed using a singular value filter (SVF) to remove the clutter signal [12] followed by MB localization [15]. A maximum intensity projection (MIP) image was then created with the values for each pixel location from 8x interpolated CEUS images. This step created high-resolution CEUS images from each imaging session. A spherical region-of-interest (ROI) of 100-pixel radius was placed on a hypoenhanced area of the tumor space (baseline images). A matched size ROI was used for all subjects. According to the mean intensity distribution as a function of time in this ROI, time-intensity curves (TICs) were created [16], [17]. Select tumor perfusion parameters were derived from TIC data, i.e. area under the curve (AUC) and peak intensity (IPK) [18]–[20].

To assess tumor microvascular morphology features, CEUS images were improved with a multiscale vessel enhancement filter, e.g. tubular structures in the image [21]. After binarization, a series of morphological image processing methods [22] were applied for computation of different structural metrics from tumor microarchitecture [23], e.g. number of branching points (NB), number of vessels (NV), mean vessel length (VL), mean vessel tortuosity (VT), mean vessel diameter (VD), and microvessel density (MVD) [11]. Note that only connected components having more than two pixels were considered as vessels for all the above-mentioned metrics.

C. Histology Analysis

Mice were euthanized and tumors were harvested after CEUS imaging at 2 h. Tumors were fixed in 10% formalin and tissue section were prepared from paraffin blocks. Sections were processed and stained for immunohistochemistry using anti-HA IgG horseradish peroxidase (HRP) conjugate and DAB substrate (Fisher Scientific, Waltham, MA). Five histology images were selected randomly from each group and used to quantify the color intensity of the HA stain.

D. Statistical Analysis

All experimental data was summarized as mean ± standard error when applicable. A linear regression analysis was performed between select functional and structural parameters. A 2-way ANOVA was used to analyze the longitudinal measurements relative to absolute baseline values from histology data. A p-value less than 0.05 was considered statistically significant.

III. RESULTS AND DISCUSSION

From our CEUS image analysis, we report the changes in tumor perfusion and microvascular morphology parameters at baseline and 2 h for all of the individual subjects. Also, TICs and ROIs from representative subjects of each group are presented in this section.

Tumor microvascular structural parameters increased at 2 h for the therapy group animals when compared to control measurements. CEUS image-based parametric values at baseline and 2 h are listed in Table 1. Two control subjects had slightly different starting values and both ended up with decreased values or no changes at 2 h after administration of saline. In contrast, the therapy subjects showed marked increased values at 2 h compared to the control group.

Figure 1 depicts the qualitative changes in tumor microarchitecture for a representative control and therapy subject, respectively. Perfusion parameters indicate a considerably higher blood volume (AUC and IPK) for the therapy group animals at 2 h after administration of PEGPH20, Figure 2.

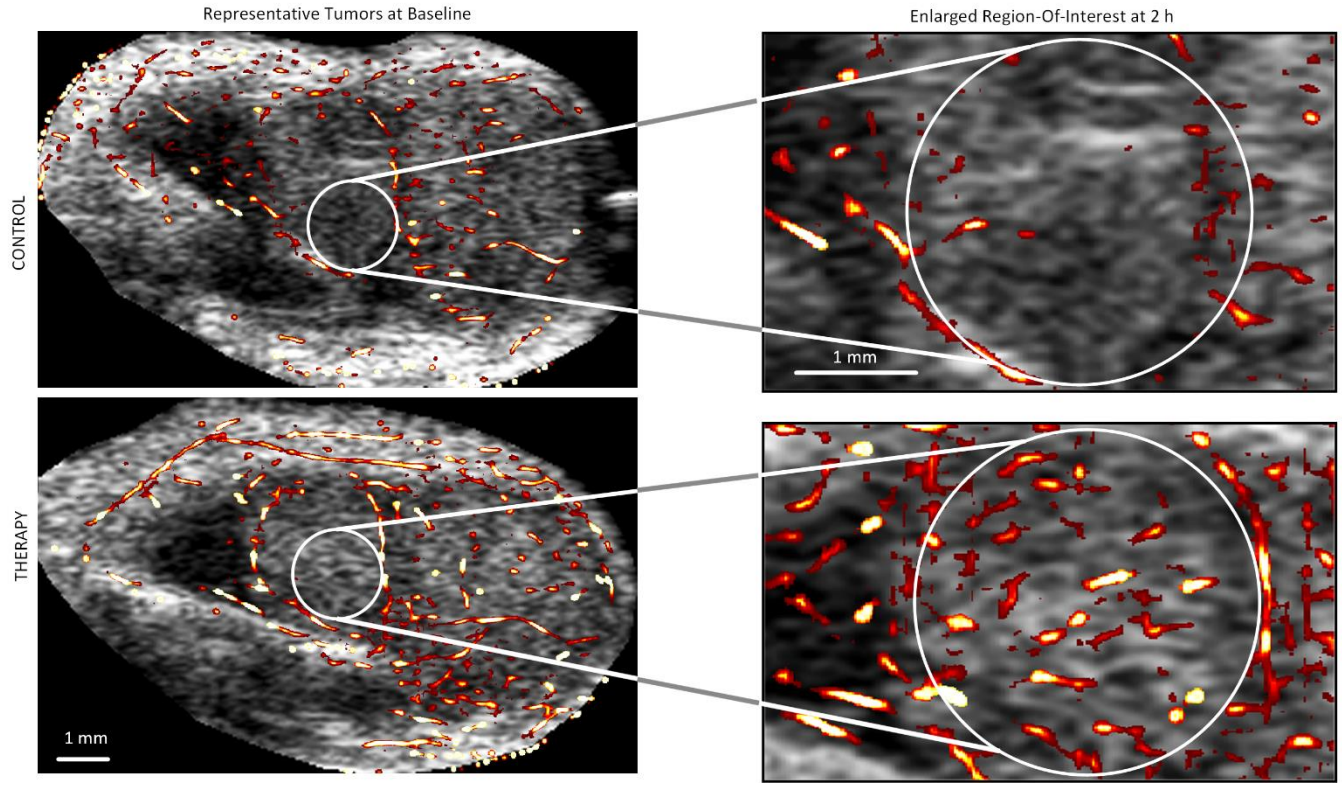

Fig. 1. B-mode ultrasound (US) images of representative pancreatic cancer-bearing mice overlaid with contrast-enhanced US (CEUS) images. Images were acquired at baseline and again at 2 h after dosing with either targeted hyaluronan (therapy, PEGPH20 drug) or saline (control). An intratumoral region-of-interest (ROI, white) was manually selected to encompass an area with relatively low tissue perfusion.

Figure 3 illustrates the linear relationship between tumor perfusion and microvascular morphology parameters. A significant correlation was observed between AUC and NV (R^2 = 0.64, p = 0.01) suggesting the amount of MBs is proportional with the number of vessels. The same is true also for the AUC and MVD parameters (R^2 = 0.58, p = 0.02). In contrast, another functional parameter IPK showed a weak correlation with the structural parameters NV (R^2 = 0.35, p > 0.10) and MVD (R^2 = 0.29, p < 0.16), respectively. After further investigation, we found that having a large vessel can produce a similar IPK value as having many small vessels. While our analysis did not discriminate based on microvessel size within the tumor ROI, if we focused our analysis on only the smaller blood vessels, we would expect an improved correlation between these CEUS image-based parametric measures. In short, these results suggest that tumors with a more extensive microvascular network have a corresponding increased tumor blood volume.

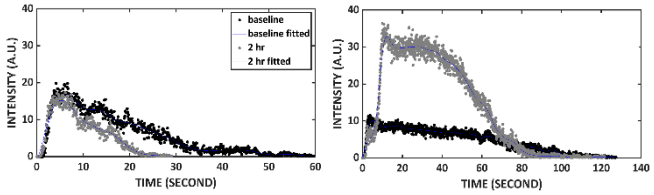

Fig. 2. Time-intensity curves (TICs) for control (left) and therapy (right) subjects. Note CEUS-derived parameter increases for the therapy group animals compared to the control group at 2 h relative to baseline.

CEUS imaging results were confirmed by histologic analysis of excised pancreatic tumor tissue samples, Figure 4. At 2 h after dosing with saline or PEGPH20, tissue samples exhibited a pronounced decrease in intratumoral HA levels when compared to control findings (p < 0.0001). Accumulation of HA is associated with the microvascular collapse and high TIP [3]. This study can be improved in a few aspects. Specifically, the accuracy of the morphological parameters can be improved by removing the motion artifacts

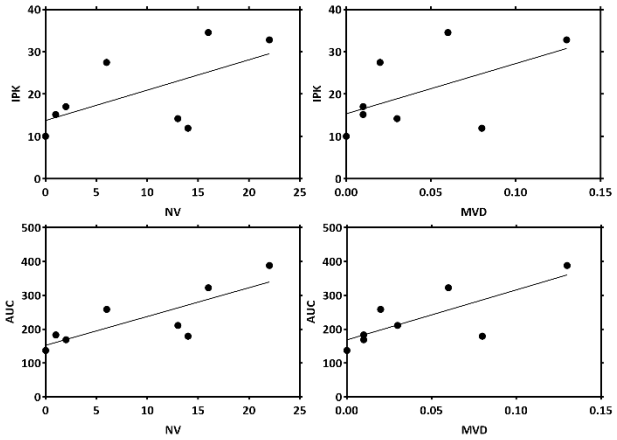

Fig. 3. Linear relationship between CEUS-derived tumor blood volume (peak intensity, IPK; area under curve, AUC) and microvascular structure (number of vessels, NV; microvessel density, MVD) at 2 h.

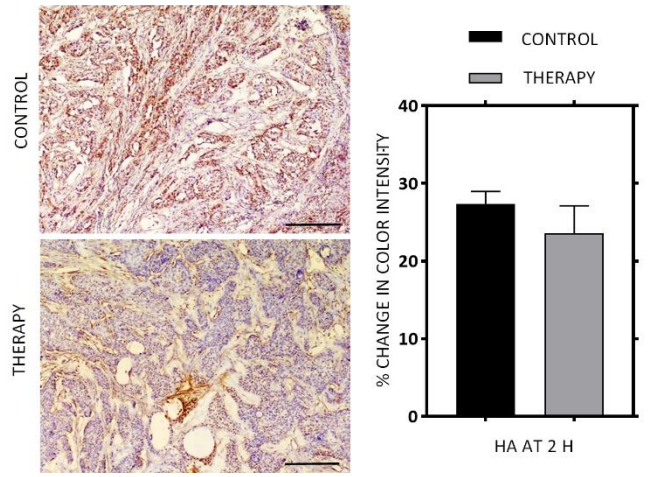

Fig. 4. Histology images from pancreatic cancer-bearing mice at 2 h after being dosed with saline (control) or PEGPH20 (therapy). Sections were stained for HA (hyaluronan) accumulation and quantified as percent tumor cross-sectional area. Scale bar = 0.5 mm.

from the images before MB localization [14]. Also, the quality of the high-resolution CEUS images could have been increased by a slower bolus injection and longer imaging sessions [13].

Previous studies have demonstrated that targeted HA degradation with PEGPH20 can help restore blood flow through previously collapsed microvascular segments and improve drug delivery [2], [5], [6]. In this study, preliminary results reveal that advantageous tumor changes after targeted HA treatment can also be monitored using CEUS images and parametric measurements of tumor perfusion and microvascular morphology.

IV. Conclusion

Monitoring acute changes in tumor perfusion and microvascular morphological features may help assess early changes such as dosing windows that are beneficial for follow up chemotherapeutic drug delivery.

References

[1] R. L. Siegel, K. D. Miller, and A. Jemal, "Cancer statistics, 2019," *CA Cancer J Clin*, vol. 69, no. 1, pp. 7–34, 2019.

[2] M. A. Jacobetz *et al.*, "Hyaluronan impairs vascular function and drug delivery in a mouse model of pancreatic cancer," *Gut*, vol. 62, no. 1, pp. 112–120, 2013.

[3] T. Stylianopoulos, L. L. Munn, and R. K. Jain, "Reengineering the physical microenvironment of tumors to improve drug delivery and efficacy: From mathematical modeling to bench to bedside," *Trends Cancer*, vol. 4, no. 4, pp. 292–319, 2018.

[4] C. B. Thompson *et al.*, "Enzymatic depletion of tumor hyaluronan induces antitumor responses in preclinical animal models," *Mol. Cancer Ther.*, vol. 9, no. 11, pp. 3052–3064, 2010.

[5] P. P. Provenzano, C. Cuevas, A. E. Chang, V. K. Goel, D. D. Von Hoff, and S. R. Hingorani, "Enzymatic targeting of the stroma ablates physical barriers to treatment of pancreatic ductal adenocarcinoma," *Cancer Cell*, vol. 21, no. 3, pp. 418–429, 2012.

[6] C. J. Whatcott *et al.*, "Desmoplasia in primary tumors and metastatic lesions of pancreatic cancer," *Clin Cancer Res*, vol. 21, no. 15, pp. 3561–3568, 2015.

[7] A. Kultti, X. Li, P. Jiang, C. B. Thompson, G. I. Frost, and H. M. Shepard, "Therapeutic targeting of hyaluronan in the tumor stroma," *Cancers (Basel)*, vol. 4, no. 3, pp. 873–903, 2012.

[8] D. Nikitovic, M. Tzardi, A. Berdiaki, A. Tsatsakis, and G. N. Tzanakakis, "Cancer Microenvironment and Inflammation: Role of Hyaluronan," *Front Immunol*, vol. 6, 2015.

[9] R. Saini and K. Hoyt, "Recent developments in dynamic contrast-enhanced ultrasound imaging of tumor angiogenesis," *Imaging Med*, vol. 6, no. 1, pp. 41–52, 2014.

[10] D. Ghosh *et al.*, "Monitoring early tumor response to vascular targeted therapy using super-resolution ultrasound imaging," in *2017 IEEE International Ultrasonics Symposium (IUS)*, 2017, pp. 1–4.

[11] I. Oezdemir and K. Hoyt, "Morphological processing for multiscale analysis of super-resolution ultrasound images of tissue microvascular networks," in *Medical Imaging 2019: Ultrasonic Imaging and Tomography*, San Diego, United States, 2019, p. 4.

[12] F. W. Mauldin, D. Lin, and J. A. Hossack, "The singular value filter: A general filter design strategy for PCA-based signal separation in medical ultrasound imaging," *IEEE Transactions on Medical Imaging*, vol. 30, no. 11, pp. 1951–1964, 2011.

[13] D. Ghosh, F. Xiong, S. R. Sirsi, P. W. Shaul, R. F. Mattrey, and K. Hoyt, "Toward optimization of in vivo super-resolution ultrasound imaging using size-selected microbubble contrast agents," *Medical Physics*, vol. 44, no. 12, pp. 6304–6313, 2017.

[14] I. Oezdemir, C. Shaw, J. R. Eisenbrey, and K. Hoyt, "Improved quantitative contrast-enhanced ultrasound imaging of hepatocellular carcinoma response to transarterial chemoembolization," in *2019 IEEE 16th International Symposium on Biomedical Imaging (ISBI 2019)*, Venice, Italy, 2019, pp. 1737–1740.

[15] C. Errico *et al.*, "Ultrafast ultrasound localization microscopy for deep super-resolution vascular imaging," *Nature*, vol. 527, no. 7579, p. 499, 2015.

[16] D. Ghosh *et al.*, "Super-resolution ultrasound imaging of the microvasculature in skeletal muscle: A new tool in diabetes research," in *2017 IEEE International Ultrasonics Symposium (IUS)*, 2017, pp. 1–4.

[17] K. Tanigaki *et al.*, "Hyposialylated IgG activates endothelial IgG receptor FcγRIIB to promote obesity-induced insulin resistance," *J Clin Invest*, vol. 128, no. 1, pp. 309–322, 2018.

[18] K. Hoyt, A. Sorace, and R. Saini, "Quantitative mapping of tumor vascularity using volumetric contrast-enhanced ultrasound," *Invest Radiol*, vol. 47, no. 3, pp. 167–174, 2012.

[19] K. Hoyt *et al.*, "Determination of breast cancer response to bevacizumab therapy using contrast-enhanced ultrasound and artificial neural networks," *J Ultrasound Med*, vol. 29, no. 4, pp. 577–585, 2010.

[20] K. Hoyt, A. Sorace, and R. Saini, "Volumetric contrast-enhanced ultrasound imaging to assess early response to apoptosis-inducing anti-death receptor 5 antibody therapy in a breast cancer animal model," *J Ultrasound Med*, vol. 31, no. 11, pp. 1759–1766, 2012.

[21] A. F. Frangi, W. J. Niessen, K. L. Vincken, and M. A. Viergever, "Multiscale vessel enhancement filtering," in *SpringerLink*, 1998, pp. 130–137.

[22] R. C. Gonzalez, R. E. Woods, and B. R. Masters, "Digital Image Processing, Third Edition," *Journal of Biomedical Optics*, vol. 14, no. 2, p. 029901, 2009.

[23] K. Hoyt, H. Umphrey, M. Lockhart, M. Robbin, and A. Forero-Torres, "Ultrasound imaging of breast tumor perfusion and neovascular morphology," *Ultrasound Med Biol*, vol. 41, no. 9, pp. 2292–2302, 2015.